

# Photon Detection Efficiency simulation of InGaAs/InP SPAD

Fabio Signorelli, Fabio Telesca, Alberto Tosi  
 Politecnico di Milano, Dipartimento di Elettronica, Informazione e Bioingegneria  
 Piazza Leonardo da Vinci 32, 20133 Milano, Italy  
 e-mail: [fabio.signorelli@polimi.it](mailto:fabio.signorelli@polimi.it)

**Abstract**—We present a comprehensive simulation flow for the estimation of photon detection efficiency as a function of wavelength in InGaAs/InP single-photon avalanche diodes (SPADs) at low temperature. We introduce a joint modelling of electrical and optical properties for SPAD detectors. We also highlight how accurately different parameters have to be calibrated in order to achieve good matching between simulations and measurements.

**Keywords**—Single-photon avalanche diode (SPAD), near-infrared detector, InGaAs/InP, photon detection efficiency, quantum efficiency, single-photon detector.

## I. INTRODUCTION

Nowadays, III-V heterostructures detectors like InGaAs/InP single-photon avalanche diodes (SPADs) are among the primary candidates for single-photon detection in the near-infrared (NIR) range, thanks to their good photon detection efficiency (PDE), low timing jitter and their ease of integration in complex real-life systems. Many applications, from eye-safe time-of-flight laser ranging (LIDAR) to quantum computing and communications, would greatly benefit from having very high PDE. So, reliable simulations of SPAD PDE are of the utmost importance for supporting the design of new detectors.

## II. DEVICE STRUCTURE

The typical “separate absorption, grading, charge and multiplication” structure of an InGaAs/InP SPAD is shown in Fig. 1 [1]. The double zinc diffusion defines the active area of the device, which includes an InP multiplication region, where carriers are multiplied by impact ionization, and an  $\text{In}_{0.53}\text{Ga}_{0.47}\text{As}$  absorption region, where the low-energy photons of interest are absorbed.

## III. PHOTON DETECTION EFFICIENCY SIMULATION

If a photon is absorbed in the InGaAs layer, an electron-hole pair is generated and the electric field drifts the hole towards the multiplication region, where an avalanche can be triggered thanks to the high electric field

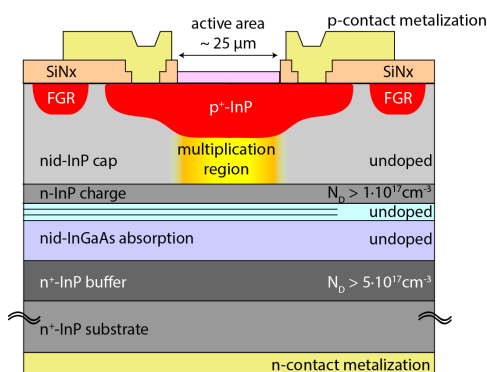


Fig. 1 - Cross-section of a typical InGaAs/InP SPAD.

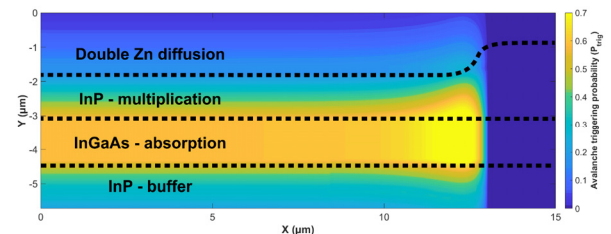


Fig. 2 – Avalanche triggering probability map when the SPAD is reverse biased 5 V beyond its breakdown voltage, i.e.  $V_{EX} = 5$  V.

( $\sim 500$  kV/cm). In order to properly estimate the photon detection efficiency of the device, two contributions have to be considered: i) the probability that an impinging photon is absorbed, i.e. the absorption probability  $P_{abs}$ ; ii) the probability that a photogenerated hole triggers a self-sustaining avalanche, i.e. the avalanche triggering probability,  $P_{trig}$ . Eventually, the photon detection efficiency is calculated as  $PDE = P_{abs} \cdot P_{trig}$  for each wavelength of interest at the operating temperature.

To this aim, we exploited both a commercial simulator (Synopsys Sentaurus) and custom-made models and scripts to manage both carrier transport and optical quantities.

### A. Electrical simulations

The model of the impact ionization coefficients in InP is crucial for correctly estimating the avalanche triggering probability. We fitted the model reported in [2] into the TCAD environment and, by following the theory of Oldham et al. [3], we calculated the probability that a photogenerated carrier injected into the high-field depleted region can trigger an avalanche. We also added carrier diffusion from the low-field quasi-neutral regions above (see Zn diffusion) and below (see InP buffer) into the depleted region. An example of the resulting avalanche triggering probability map with all the contributions is reported in Fig. 2.

### B. Optical simulations

Bidimensional optical simulations based on geometrical optics, such as raytracing, or transfer-matrix methods are not well suited for estimating the photon absorption in InGaAs/InP SPADs, since the thickness of the different layers of the structure is comparable to the wavelength of interest ( $0.8 - 1.7 \mu\text{m}$ ). So, we employed the finite difference time domain (FDTD) method to directly solve Maxwell’s equations inside the device. FDTD simulations would require the whole 3D SPAD structure, thus leading to very long simulations. However, we verified that, for sufficiently large active area diameters ( $> 10 \mu\text{m}$ ), a 2D simulation along a cross-section leads to very similar results at a fraction of the computational effort. Our model includes the complete back-end material stack, such as metal lines, nitrides and oxides. Fig. 3 shows exemplary simulation results at  $\lambda = 1550$  nm. Ray tracing and transfer-matrix simulations would not report all the interference patterns visible in the absorption layer.

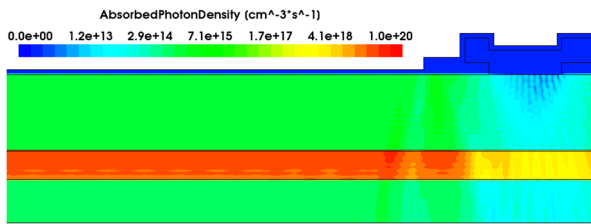


Fig. 3 – FDTD optical simulation results at  $\lambda = 1550$  nm: absorbed photon density in a SPAD cross-section with  $1 \text{ mW/cm}^2$  illumination.

### C. Parameter calibration

Given the uncertainties inherent in the fabrication processes, an accurate calibration of TCAD models with experimental data is required in order to reliably estimate all the parameters having an impact on PDE.

Concerning the electrical properties of InP, ionization coefficients models must be calibrated at the electric fields and temperatures at which the SPAD operates. In order to estimate the electric field, accurate doping concentration can be determined from experimental measurements, with more focus on the regions where the electric field changes sharply, i.e. the zinc diffusion and the charge layer.

Minority carriers lifetime  $\tau_c$  in the zinc diffusion region has to be properly estimated, as well as its dependence on doping concentration: we determined that  $\tau_c$  is in the range of hundreds of picoseconds, in agreement with [4].

Concerning optical parameters, the complex refractive index for both InP and InGaAs have been measured and reported in the literature in the past decades, but data are not complete and often conflicting each other. Hence, a proper choice of datasets has been carried out, based on the reported measurement condition: InP complex refractive index reported in [5] was chosen, since it resulted from a comparison among different sets, based on the experimental technique and its limitations. Its dependence on temperature was taken from [6]. Regarding InGaAs, in the 1-1.4  $\mu\text{m}$  wavelength range all the available models present very similar results, while at longer wavelengths we considered the results from [7], where absorption coefficients were accurately measured at various temperatures. Then, we calculated the refractive index of InGaAsP layers with a linear interpolation from the ones of InP and InGaAs [8].

InGaAs/InP SPADs usually work far below room temperature, from 240 K down to 200 K. Since the temperature dependence of many parameters is not well assessed in the literature, we extrapolated missing values of some parameters from existing data. The precise estimation of the absorption coefficients and their dependence on temperature, for both InP and InGaAs, is particularly critical, as it defines the cutoff wavelengths for both materials. At typical operating temperature ( $\sim 200$  K), the cutoff wavelength of InP and InGaAs are around 910 nm and 1.6  $\mu\text{m}$ , respectively.

Fig. 4 shows the photon detection efficiency obtained from simulations, compared to an experimentally measured one. In the 0.9-1  $\mu\text{m}$  wavelength range, the residual error between simulated and measured curves could be due to either the estimation of the InP cutoff wavelength at 200 K or to a small temperature error in the measurement setup. From 1  $\mu\text{m}$  to 1.4  $\mu\text{m}$ , simulated PDE values are very close to experimental ones, while at long wavelengths ( $> 1.4$   $\mu\text{m}$ ) the reason for the visible difference could be twofold: i) an inaccurate modelling of the InGaAs absorption coefficient around its cutoff wavelength ( $\sim 1.6$   $\mu\text{m}$ ) at 200 K; ii) photons absorbed in the InGaAs layer surrounding the depleted region that diffuse towards the central active area

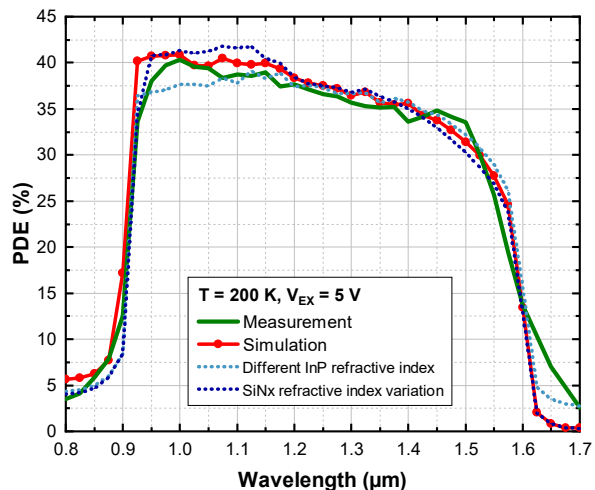


Fig. 4 – Experimental and simulated photon detection efficiency as a function of wavelength. Up to 900 nm, InP prevents most of the photons from reaching the high triggering probability regions. Dotted lines show that small changes in some parameters can have a visible impact.

and are then able to trigger an avalanche [9]. Further investigations on this process are ongoing.

Finally, the small oscillations in the simulated PDE curves are slightly different compared to measured ones due to minor differences in either layer thickness or composition of either the nitrides, acting as antireflection coating on top of the active area, or the InGaAsP layer. Fig. 4 reports also two additional simulations: one where the SiNx refractive index is slightly changed (10 % w.r.t. nominal value) as if the composition of the nitride is not the reference one, while in the second one the InP absorption coefficient is overestimated, thus giving lower PDE at short wavelengths, because photons are not anymore absorbed in the high avalanche triggering probability InGaAs layer.

### REFERENCES

- [1] A. Tosi, N. Calandri, M. Sanzaro, and F. Acerbi, “Low-noise, low-jitter, high detection efficiency InGaAs/InP single-photon avalanche diode,” *IEEE J. Sel. Top. Quantum Electron.*, vol. 20, no. 6, 2014.
- [2] F. Zappa, P. Lovati, and A. Lacaita, “Temperature dependence of electron and hole ionization coefficients in InP,” in *Conference Proceedings - International Conference on Indium Phosphide and Related Materials*, 1996, pp. 628–631.
- [3] W. G. Oldham, R. R. Samuelson, and P. Antognetti, “Triggering Phenomena in Avalanche Diodes,” *IEEE Trans. Electron Devices*, vol. 19, no. 9, pp. 1056–1060, 1972.
- [4] J. A. Yater, I. Weinberg, P. P. Jenkins, and G. A. Landis, “Minority-carrier lifetime in InP as a function of light bias,” in *Conference Record of the IEEE Photovoltaic Specialists Conference*, 1994, vol. 2, pp. 1709–1712.
- [5] E. D. Palik, *Handbook of Optical Constants of Solids, Five-Volume Set*. Academic Press, 1997.
- [6] W. J. Turner, W. E. Reese, and G. D. Pettit, “Exciton Absorption and Emission in InP,” *Phys. Rev.*, vol. 136, no. 5A, p. A1467, Nov. 1964.
- [7] E. Zielinski, H. Schweizer, K. Streubel, H. Eisele, and G. Weimann, “Excitonic transitions and exciton damping processes in InGaAs/InP,” *J. Appl. Phys.*, vol. 59, no. 6, pp. 2196–2204, 1986.
- [8] S. Seifert and P. Runge, “Revised refractive index and absorption of  $\text{In}_{1-x}\text{Ga}_x\text{As}_y\text{P}_{1-y}$  lattice-matched to InP in transparent and absorption IR-region,” *Opt. Mater. Express*, vol. 6, no. 2, p. 629, Feb. 2016.
- [9] N. Calandri, M. Sanzaro, A. Tosi, and F. Zappa, “Charge Persistence in InGaAs/InP Single-Photon Avalanche Diodes,” *IEEE J. Quantum Electron.*, vol. 52, no. 3, Mar. 2016.